Journal of Polymers and the Environment (2026) 34:21
https://doi.org/10.1007/s10924-025-03753-8

ORIGINAL PAPER

Joncryl Chain Extender Reactivity with Polylactide: Effect of PLA Molecular Weight and the Resultant Rheological and Crystallization Behaviors

Yavuz Akdevelioğlu[1] · M. Begum Alanalp[2] · Jed Randall[3] · Michael Gehrung[3] · Ali Durmus[2] · Davoud Jahani[4] · Mohammadreza Nofar[1]

Received: 10 June 2025 / Accepted: 5 November 2025
© The Author(s) 2026

Abstract

This study investigates the effect of polylactide (PLA) molecular weight on the reactivity of multifunctional epoxy-based chain extender, Joncryl. PLA samples with low (L-PLA), medium (M-PLA), and high (H-PLA) molecular weights, each with D-lactic acid contents below 1.5 mol%, were melt-processed with 0.5 and 1.0 wt% Joncryl ADR 4468. The melt rheological behavior, molecular weight, and crystallization kinetics of the processed samples were evaluated using a rheometer, gel permeation chromatography (GPC), and differential scanning calorimetry (DSC), respectively. Small-amplitude oscillatory shear rheology and GPC analyses showed that Joncryl reactions with higher molecular weight PLA resulted in more dramatic enhancements. This enhanced long-chain branching in turn provided stronger improvements to the melt rheological properties and to final molecular weight. Non-isothermal DSC analysis demonstrated that Joncryl modification suppressed crystallization more noticeably in high-molecular weight PLAs. Isothermal DSC analysis further revealed that long-chain branching nearly doubled the crystallization time while significantly reducing the final crystallinity.

Keywords Polylactide · Molecular weight · Joncryl · Rheology · Differential scanning calorimetry

Introduction

The widespread use of petroleum-based polymers has raised significant environmental concerns, creating a strong demand for bio-based and biodegradable alternatives such as polylactide (PLA) [1, 2]. However, the application of PLA in commodity and engineering products is limited by several shortcomings, including low thermal stability, low melt strength, slow crystallization, and poor processability [3–13]. Chemical modification using suitable chain extenders has been demonstrated as a practical and effective approach to address these limitations [14–36]. Linear chain extension can improve properties such as melt strength and thermal stability. Nevertheless, the introduction of branched

✉ Davoud Jahani
davoud@ubonab.ac.ir

✉ Mohammadreza Nofar
nofar@itu.edu.tr

Yavuz Akdevelioğlu
akdevelioglu@itu.edu.tr

M. Begum Alanalp
begumalanalp@gmail.com

Jed Randall
bioplasticman1@gmail.com

Michael Gehrung
mike_gehrung@natureworksllc.com

Ali Durmus
durmus@iuc.edu.tr

[1] Sustainable & Green Plastics Laboratory, Metallurgical & Materials Engineering Department, Faculty of Chemical and Metallurgical Engineering, Istanbul Technical University, Istanbul 34469, Turkey

[2] Department of Chemical Engineering, Faculty of Engineering, Istanbul University-Cerrahpasa, Avcılar, Istanbul 34320, Turkey

[3] NatureWorks LLC, Plymouth, MN, USA

[4] Mechanical Engineering Department, Faculty of Engineering, University of Bonab, Bonab, Iran

Published online: 12 January 2026

structures has been shown to be considerably more effective in enhancing these characteristics. Both chain extension and branching contribute to an increase in molecular weight. However, in comparison with linearly extended molecules, branched structures exhibit superior thermal stability and melt rheological performance [27, 37, 38].

McKee et al. [14], Götterman et al. [16], and Meng et al. [28] demonstrated that the use of various chain extenders significantly increases the complex viscosity of modified PLA as a result of chain extension and branching. Chain extenders were also shown to effectively counteract the thermal degradation of PLA [22, 28]. Among different types of chain extenders, multifunctional epoxy-based Joncryl has been studied extensively due to its high reactivity, particularly with polyester-based polymers [39–41]. The incorporation of Joncryl substantially enhances the melt rheological properties of polyesters by increasing molecular weight and inducing chain branching [42–45]. Consequently, Joncryl modification improves both the processability and the foaming ability of polyesters [18, 19, 25, 30, 41]. In our previous study [26], the effect of PLA D-lactic acid content (D-content) on the reactivity of two Joncryl grades (4468 and 4400) under different processing temperatures was comprehensively investigated. The results revealed that Joncryl reactivity increased at higher processing temperatures. Furthermore, Joncryl 4468 exhibited more effective chain extension and branching than Joncryl 4400, owing to its higher functionality. A wide variation in D-content (0.5 vs. 12 mol%) also led to certain differences in the preference for chain extension versus branching in PLA samples.

The use of Joncryl can also influence the crystallization kinetics of PLA in different ways. Nofar et al. [20] and Bai et al. [46] reported that long-chain branching can enhance crystallization, as branches may serve as anchoring sites for additional crystal nucleation. However, when the Joncryl content exceeds a certain threshold, crystallization of the final product may be significantly hindered [21]. As the degree of branching increases, both disrupted molecular symmetry and the associated rise in molecular weight interfere with crystallization kinetics [20, 26]. It should be emphasized that the crystallization behavior of PLA is strongly dependent on the D-content within the polymer chain. PLAs with lower D-content crystallize more rapidly due to higher molecular symmetry, which allows greater levels of crystallinity to be achieved. In contrast, PLAs with higher D-contents exhibit disrupted molecular symmetry, which directly suppresses both crystal perfection and crystallization rate. As a result, PLAs with zero D-content can achieve melting temperatures around 180 °C, whereas PLAs with D-contents beyond 8 mol% are fully amorphous [47, 48]. Molecular weight also affects the crystallizability of PLA [49, 50]. An increase in molecular weight generally reduces chain mobility and thus limits crystallization [51]. Conversely, molecular weight reduction through degradation has been reported to increase both the crystallization rate and the degree of crystallinity in various PLA grades [13, 52]. Therefore, the interaction of Joncryl with different PLA types—varying in molecular weight, configuration, and structure—can differently influence crystallization behavior. The extent of chain extension and branching, as well as the molecular synergy created, ultimately determines the outcome of crystallization.

Although numerous studies have investigated the use of different chain extenders, including various grades of Joncryl with a wide range of PLA grades, the correlation between PLA molecular structure and Joncryl reactivity has not been fully clarified. Building upon our earlier work [26], in which the influence of PLA D-lactic acid content on Joncryl reactivity at different processing temperatures was examined, the present study focuses on the effect of PLA molecular weight on Joncryl reactivity. This objective is pursued through comprehensive investigations of melt rheology and crystallization behavior. For this purpose, three PLA grades with different molecular weights possessing D-contents below 1.5 mol% were melt compounded with 0.5 and 1.0 wt% Joncryl 4468. Small amplitude oscillatory shear (SAOS) and extensional rheological analyses were used to evaluate melt characteristics. Gel permeation chromatography (GPC) was used to verify the molecular weight variations of the processed samples. Differential scanning calorimetry (DSC) was used to determine the non-isothermal and isothermal crystallization behaviors of the modified PLAs.

Experimental

Materials and Sample Preparation

Three commercial PLA grades with different molecular weights (i.e., low, medium and high) were supplied from NatureWorks LLC. These grades were Ingeo 3251D, 3001D, and 2500HP, corresponding to low (L-PLA), medium (M-PLA), and high (H-PLA) molecular weights, respectively [12]. The D-lactic acid contents of these polymers were all below 1.4 mol%. The detailed specifications of these PLAs are given in Table 1.

The chain extender used was an oligomeric multifunctional epoxy-based Joncryl ADR 4468 (BASF, Germany), which has a molecular weight of 7250 g/mol and an epoxide equivalent weight of 310 g/mol, corresponding to a weight-average functionality of approximately 23 [41]. Prior to processing, both PLA and Joncryl were vacuum-dried at 50 °C overnight. Melt processing was carried out with Joncryl

Table 1 Properties of PLA grades according to supplier specifications

PLA Grades	Mw (g/mol)	D-Content (mol%)	Melting Point (°C)	Melt Flow Rate (g/10min @210°C)
3251D	100,000	1.4	155–170	80
3001D	138,000	1.4	160–170	22
2500HP	192,000	0.5	165–180	8

contents of 0.5 and 1.0 wt% using an internal melt mixer (Kökbir Ltd. Şti.) at 190 °C and 100 rpm for 5 min. Disc-shaped samples for rheological testing were then prepared by compression molding at 1.5 tons for 5 min. During molding, the pressure was gradually increased at 30-second intervals. The samples were rapidly water-cooled to room temperature before release.

Rheological Analysis

The SAOS rheological analysis of the unmodified and Joncryl modified L-PLA, M-PLA, and H-PLA samples were conducted using a rotational rheometer (MCR-301, Anton Paar, Austria) with parallel plates (25 mm diameter, 1 mm gap). The strain amplitude was set at 5.0% for unmodified PLAs and 1.0% for Joncryl modified samples, that were within the linear viscoelastic region. Frequency sweep experiments were performed from high to low frequency to examine the effect of Joncryl reactivity on the complex viscosity and moduli values. In addition, time sweep experiments were carried out for 20 min at the same strain amplitudes and a frequency of 1.0 rad/s. All measurements were performed at 190 °C. Carreau–Yasuda fitting and time-weighted relaxation spectra models and Cole–Cole and Van Gurp–Palmen plots were also used for more in depth analyses. Details of these models and the corresponding calculations are available elsewhere [26].

Extensional rheological analysis of all unmodified and Joncryl modified samples were carried out with RDA III rheometer from TA Instruments (New Castle, OH, USA). L-PLA and M-PLA samples were measured at 165 °C, whereas H-PLA samples were measured at 175 °C.

Gel Permeation Chromatography (GPC)

GPC was utilized to determine the molecular weights of both unmodified and Joncryl modified samples. The reported molecular weight values were calibrated against narrow polystyrene standards. For sample preparation, approximately 0.5 ± 0.02 g of material was dissolved in 9.5 mL of solvent, with methylene chloride used for all samples. A 0.25 mL portion of this solution was further diluted with 5 mL of tetrahydrofuran (THF) and subsequently filtered using a 0.45-micron PTFE syringe filter. The analysis was conducted using a Waters 2695 separations module, which injected 100 µL of the prepared solution while maintaining a THF mobile phase flow rate of 1.0 mL/min. The separation process was carried out using three Waters Styragel HR columns (5 µm particle size, 300 mm × 7.8 mm), arranged in series with pore sizes of 10^5 Å (HR-5), 10^4 Å (HR-4), and 10^1 Å (HR-1). Both the column set and the detector were maintained at a constant temperature of 35 °C. A Waters 410 differential refractometer was employed as the detector. Data acquisition and processing were performed using Millennium version 3.2 software, with the polymer peak integration limited by a low molecular weight cutoff set at the retention volume corresponding to a 4000 g/mol polystyrene standard.

Differential Scanning Calorimetry (DSC) Analysis

DSC analysis was conducted using a SII Nanotechnology DSC 6200. All DSC runs were carried out under nitrogen (N_2) atmosphere with a flow rate of 50 ml/min. For the non-isothermal analysis, samples were first heated to 200 °C at a rate of 10 °C/min and held at this temperature for 3 min to erase their thermal history. They were then cooled to room temperature either at a slow rate (2 °C/min) to maximize crystallization or at a fast rate (30 °C/min) to avoid melt crystallization during cooling and explore cold crystallization during the second heating. Subsequently, the samples were reheated to 200 °C at 10 °C/min. The degree of crystallinity, calculated from the heat flow (X_c^{heat}), was calculated using the heat of fusion values for 100% crystalline PLA (ΔH°_m = 93.6 J/g) [20, 53] according to Eq. 1 [54]:

$$X_c^{heat} = \frac{(\Delta H_m - \Delta H_{cc}) \times 100}{w_{PLA} \Delta H_m^0} \quad (1)$$

where W_{PLA} refers to the weight fraction of PLA and ΔH_m and ΔH_{cc} refer to heat enthalpy of melting and cold crystallization, respectively. The heat enthalpy of melt crystallization during the cooling cycle is also reported as ΔH_c.

For the isothermal analysis, all samples were heated to 200 °C at a rate of 20 °C/min and held at this temperature for 3 min to remove their thermal history and melt all crystals. They were then cooled to the isothermal temperatures of 90, 100, 110, and 120 °C at a cooling rate of 30 °C/min. Crystallization kinetics were evaluated using the Avrami model [55].

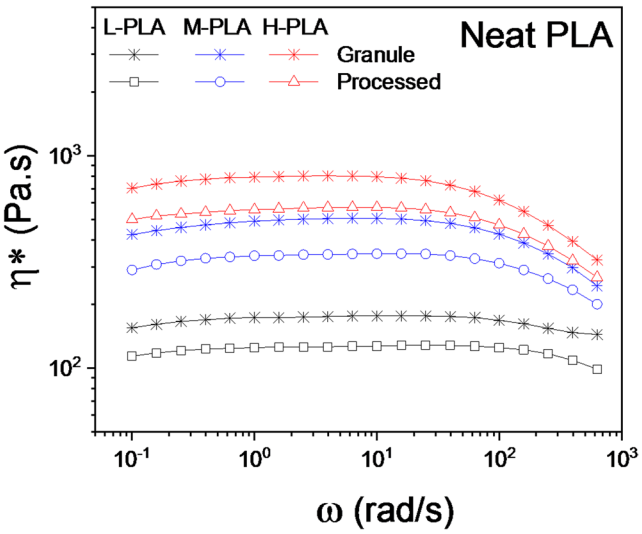

Fig. 1 Complex viscosity versus angular frequency of unprocessed (granule) and melt processed neat PLA samples, measured at 190 °C

Table 2 Complex viscosity at 0.1 rad/s and molecular weight of granule and processed samples

Samples	$\eta^*_{0.1}$(Pa.s)	Measured Mw (g/mol)
L-PLA		
Granule	155	88,500
Processed	114	79,564
M-PLA		
Granule	426	118,000
Processed	290	107,963
H-PLA		
Granule	704	136,000
Processed	501	124,473

Results and Discussion

Shear Rheological Analysis

Figure 1 presents the complex viscosity (η*) as a function of angular frequency (ω) for unprocessed granules and processed neat PLA samples. Numerical values of complex viscosity and the corresponding molecular weights are provided in Table 2. The order of complex viscosity for different PLA grades clearly reflects their molecular weight hierarchy: L-PLA<M-PLA<H-PLA. It was observed that melt processing reduced the molecular weight in all PLA samples due to thermal degradation, resulting in lower complex viscosity across the entire frequency range. Additionally, a slight decrease in complex viscosity was noted at low frequencies (< 1.0 rad/s) following the Newtonian plateau, which can be attributed to further thermal degradation occurring during the rheological measurement from high to low frequency.

Figure 2 compares the frequency sweep rheological behavior of processed unmodified PLAs with their Joncryl modified counterparts. The Carreau–Yasuda fitted results are presented in Fig. 2a, while Fig. 2b shows the normalized complex viscosity values to better illustrate the effect of Joncryl on PLAs with different molecular weights. Table 3 provides both the zero-shear viscosity values obtained from the Carreau–Yasuda model and the experimentally measured complex viscosities at 0.1 rad/s. It should be noted that experimental values at 0.1 rad/s are expected to be slightly lower than the model predictions due to thermal degradation during analysis. The addition of Joncryl, and increasing its content, led to higher complex viscosities in all PLA samples, particularly at lower frequencies. This increase was more pronounced in PLAs with higher molecular weights, reflecting the formation of longer chain branches between Joncryl and high-molecular-weight PLA. While the complex viscosity of modified L-PLA showed the smallest increase, that of modified H-PLA exhibited the largest increase across a broader frequency range. Consequently, shorter branches in L-PLA result in weaker branch interactions, whereas longer branches in H-PLA form stronger physical entanglements, leading to a more substantial enhancement in melt properties. This effect is evident in Fig. 2b, where Joncryl modification increased complex viscosity by approximately 15-fold in L-PLA and around 30-fold in H-PLA compared to their unmodified counterparts. Longer chain branching in higher-molecular-weight PLAs is further illustrated in Fig. 2c. In terms of storage modulus (G′), neat PLA samples exhibited a terminal zone slope close to 2, consistent with linear chain structures [16, 30, 56]. The slope in the terminal zone decreased further upon increasing long-chain branching, particularly in high-molecular-weight PLAs modified with 1.0 wt% Joncryl. This decrease was most pronounced in H-PLA, reflecting the formation of longer branches with stronger physical interactions, whereas shorter branches in L-PLA resulted in weaker molecular entanglements.

Figure 3 presents the time-weighted relaxation spectra (λH(λ)) as a function of relaxation time (λ) for all processed samples and the corresponding relaxation time values at the peaks are reported. Neat PLA samples either exhibit no relaxation peak (e.g., unmodified L-PLA) or a peak at very short relaxation times (< 0.01 s). This behavior corresponds to very weak physical interactions, where liquid-like behavior dominates with minimal solid-like response, as typically observed for relaxation times below 1.0 s. In contrast, Joncryl modification shifts the relaxation peak to longer times, indicating stronger physical interactions and more pronounced solid-like behavior [30]. In modified L-PLA, the formation of shorter-range branches results in lower relaxation times, and liquid-like behavior remains dominant

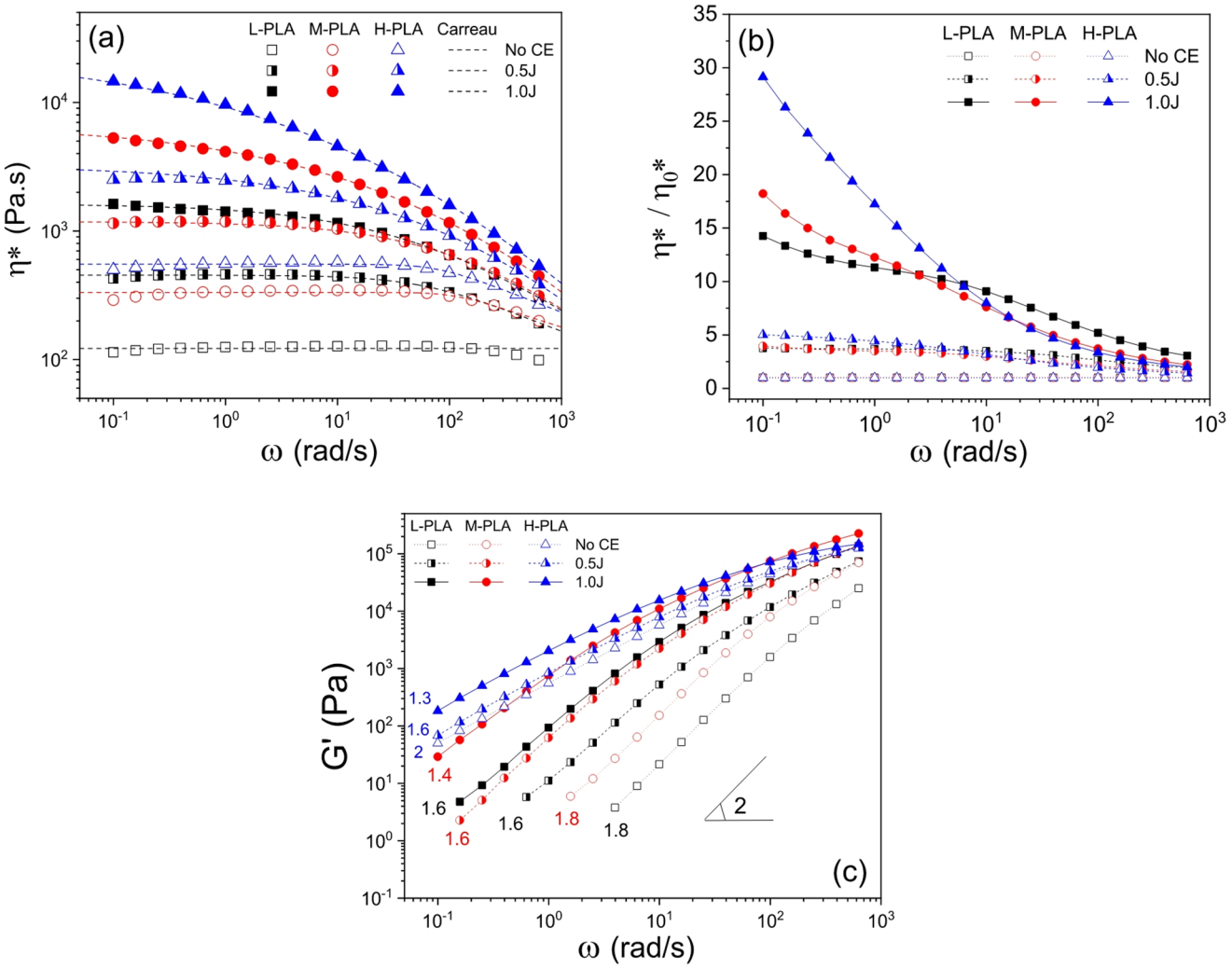

Fig. 2 (**a**) complex viscosity with Carreau-Yasuda fitting, (**b**) normalized complex viscosity and (**c**) storage modulus versus frequency of all processed samples, measured at 190 °C

Table 3 Complex viscosity at 0.1 rad/s from experimental values and zero-shear viscosity values calculated from Carreau-Yasuda model fitting

Samples	$\eta^*_{0.1}$(Pa.s)	η^*_0(Pa.s) (Carreau-Yasuda)
L-PLA		
No CE	113	122
0.5 J	426	453
1.0 J	1623	1623
M-PLA		
No CE	290	333
0.5 J	1147	1181
1.0 J	5286	6756
H-PLA		
No CE	501	551
0.5 J	2510	3242
1.0 J	14,600	24,978

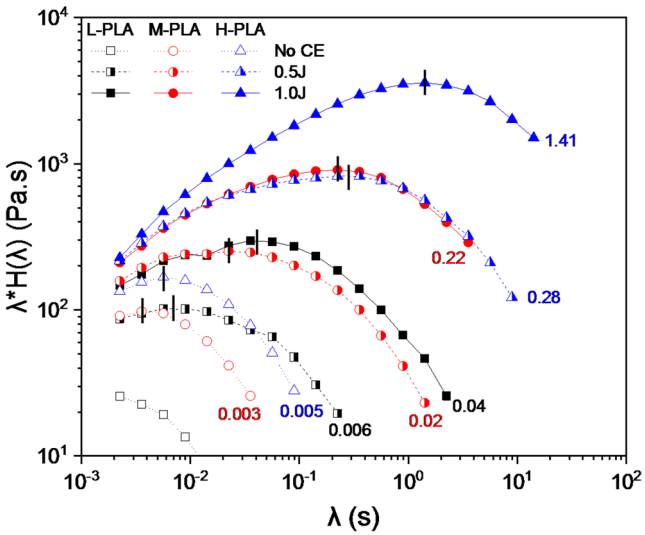

Fig. 3 Time-weighted relaxation spectra and their corresponding relaxation peak values of the processed samples

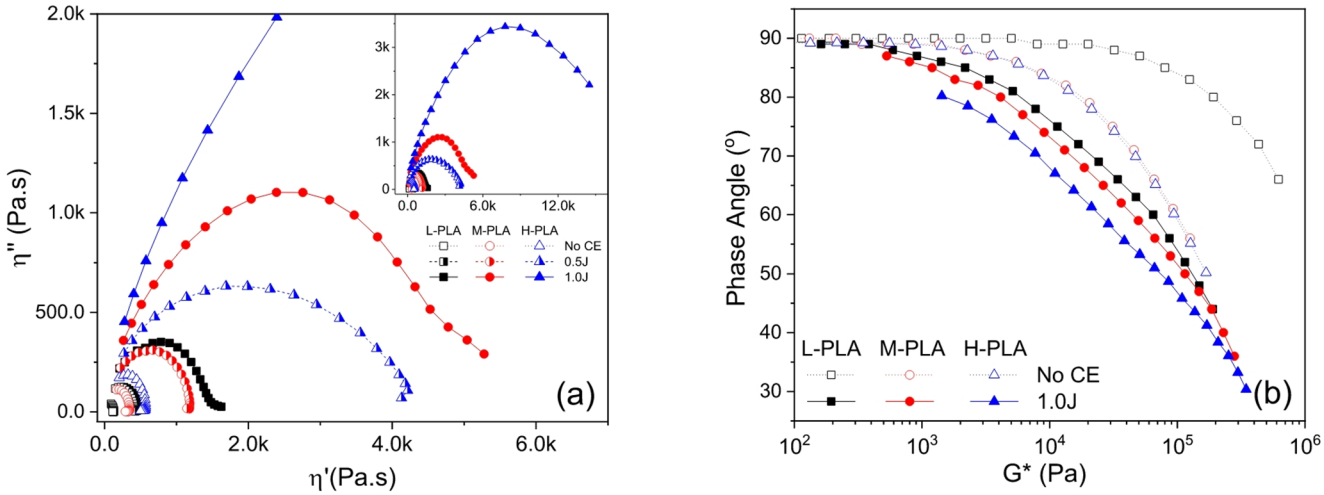

Fig. 4 (**a**) Cole-Cole and (**b**) Van-Gurp Palmen plots of all processed samples

even at 1.0 wt% Joncryl. For H-PLA, however, the relaxation peak shifts more substantially toward longer times with increasing Joncryl content, reflecting stronger physical interactions due to longer chain branches. The effect of branching is particularly pronounced in higher-molecular-weight PLAs. For example, the relaxation times of neat M-PLA and H-PLA are approximately 0.003 s and 0.005 s, respectively. Upon modification with 0.5 wt% Joncryl, these values increase to around 0.02 s and 0.28 s, and further rise to approximately 0.22 s and 1.41 s at 1.0 wt% Joncryl. Corresponding relaxation times in L-PLA modified with 0.5 and 1.0 wt% Joncryl are 0.006 s and 0.04 s, respectively. These substantial increases in molecular relaxation times for high-molecular-weight PLAs clearly indicate the formation of long-chain branches and the associated enhancement of molecular entanglements.

Figure 4 presents the Cole–Cole and Van Gurp–Palmen plots derived from the frequency sweep data. In Fig. 4a, the Cole–Cole plots of unmodified PLAs form incomplete circular patterns, with increasing molecular weight resulting in slightly larger diameters. In contrast, Joncryl-modified samples exhibit a much more pronounced increase in the diameter of the incomplete circles and deviate from the semicircular pattern. As reported in the literature [30], such increases in diameter combined with deviations from circularity indicate the presence of long-chain branched structures. For L-PLA, the effect of long-chain branching on relaxation was considerably smaller compared to H-PLA. This observation supports the conclusion that molecular weight plays a significant role in relaxation behavior once long-chain branches are introduced. To further illustrate differences in chain structure before and after Joncryl modification, changes in the phase angle (δ) as a function of complex shear modulus (G*) are shown in Fig. 4b. A reduction in phase angle indicates longer relaxation times due to branching or higher polydispersity [16, 56]. Although Joncryl modification caused a similar increase in polydispersity across all samples (Table 4), the phase angle change was most pronounced in H-PLA. This suggests a correlation between the initial molecular weight of PLA and the strength of branch interactions.

Table 4 Molecular weight values of processed samples from experimental values through GPC and calculated values through modified power-law model

Samples	Measured Mw (g/mol)	Apparent Mw (g/mol)	Polydispersity Index (PDI)
L-PLA			
No CE	79,564	64,232	1.66
0.5 J	167,625	92,784	2.68
1.0 J	220,159	137,508	2.72
M-PLA			
No CE	107,963	86,300	1.81
0.5 J	190,567	125,233	2.56
1.0 J	266,444	209,168	2.56
H-PLA			
No CE	124,473	100,078	1.91
0.5 J	233,327	168,542	2.77
1.0 J	327,335	307,267	2.93

Figure 5 presents the time sweep rheological analysis of unmodified and Joncryl modified PLA samples. Thermal degradation resulted in a reduction of complex viscosity in all unmodified PLA samples. In contrast, the addition of Joncryl appears to mitigate the effects of thermal degradation by promoting chain extension and branching. The initial molecular weight of the samples had little effect on thermal degradation, as all unmodified PLAs exhibited a similar loss in complex viscosity. The relatively gradual change in complex viscosity over time in the Joncryl-modified samples suggests that most of the Joncryl reactions were completed

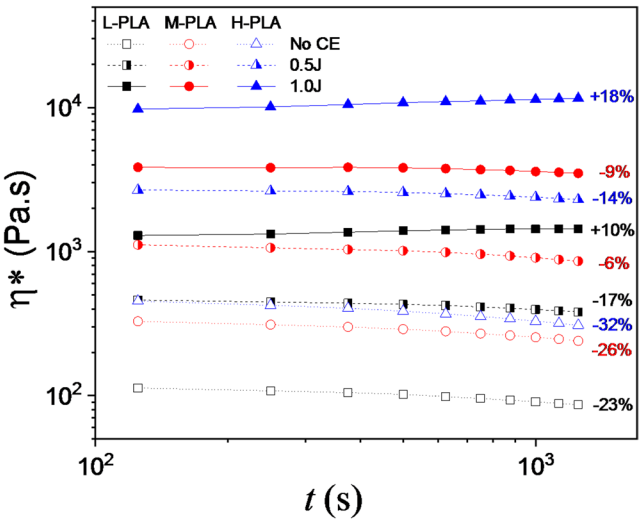

Fig. 5 Time versus complex viscosity of all processed samples, measured at 190 °C

during melt processing. Any residual Joncryl molecules likely contributed to compensating for further molecular degradation.

Extensional Rheological Analysis

Figure 6 presents the extensional rheological analysis of M-PLA (Fig. 6a) and H-PLA (Fig. 6b) samples. Due to the very low extensional viscosity of L-PLA, both before and after Joncryl modification, reliable data could not be obtained. This observation highlights the significant effect of initial molecular weight on extensional viscosity, as low molecular weight results in weaker physical entanglements. Consequently, branch interactions in Joncryl-modified L-PLA are also weaker, consistent with the trends observed in Figs. 3 and 4. The impact of initial molecular weight is further evident when comparing Joncryl-modified M-PLA and H-PLA. H-PLA exhibited higher extensional viscosity overall and earlier onset of strain hardening than M-PLA. In unmodified samples, H-PLA displayed lower extensional viscosity compared to M-PLA, and the onset of sagging was more pronounced. This behavior is attributed to the lower D-content in H-PLA, which reduces the strength of physical entanglements, as discussed in our previous study [26].

GPC Analysis

Figure 7 presents the GPC analysis results of unmodified and Joncryl-modified PLA samples. Table 4 reports the molecular weight values obtained from GPC, as well as the apparent molecular weights determined from rheological analysis [22, 26, 57]. The mathematical model used to calculate apparent molecular weight (Equation S1) and full GPC chromatograms (FigureS1-3) are also provided in the Supplementary Data. Joncryl-modified samples exhibited higher molecular weights and increased polydispersity index (PDI) values, resulting from branching reactions that convert linear molecules into very high-molecular-weight species with a broader distribution. After modification, L-PLA retained the lowest molecular weight due to its initially low molecular weight, whereas H-PLA achieved the highest molecular weight. As shown in Fig. 7a, the increase in molecular weight is more pronounced for PLAs with higher initial molecular weight upon Joncryl addition, which is consistent with the trends observed in the rheological analyses of the processed samples.

DSC Analysis

Figure 8 shows the second heating thermograms of fast-cooled, processed unmodified and Joncryl-modified PLA samples, and Table 5 summarizes the corresponding thermal properties. Cooling was performed at a rate of 30 °C/min, which suppresses PLA crystallization due to its inherently slow crystallization kinetics (data not shown). Consequently, crystallization takes place during the subsequent heating cycle in the form of cold crystallization. The low D-content of H-PLA allowed both crystallinity and crystal melting temperatures to be higher than in other PLAs. Despite its higher molecular weight, H-PLA exhibits higher crystallinity and crystal melting temperatures than L-PLA and M-PLA, as its low D-content promotes chain conformity which promotes higher crystallizability [10]. A small

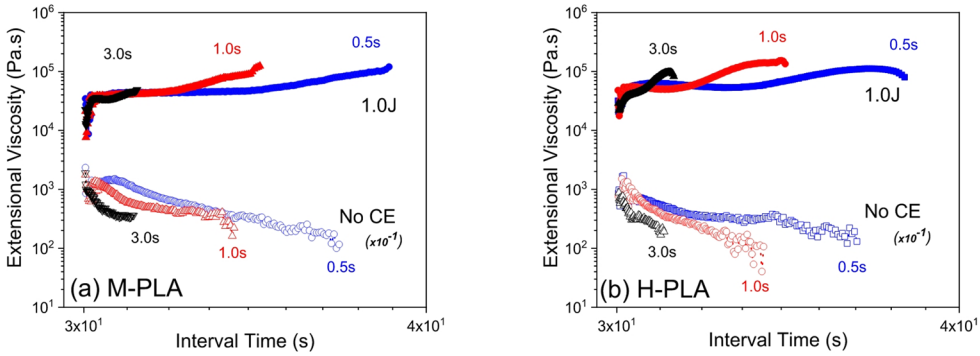

Fig. 6 Extensional viscosity versus time of neat and Joncryl modified (**a**) M-PLA and (**b**) H-PLA processed samples

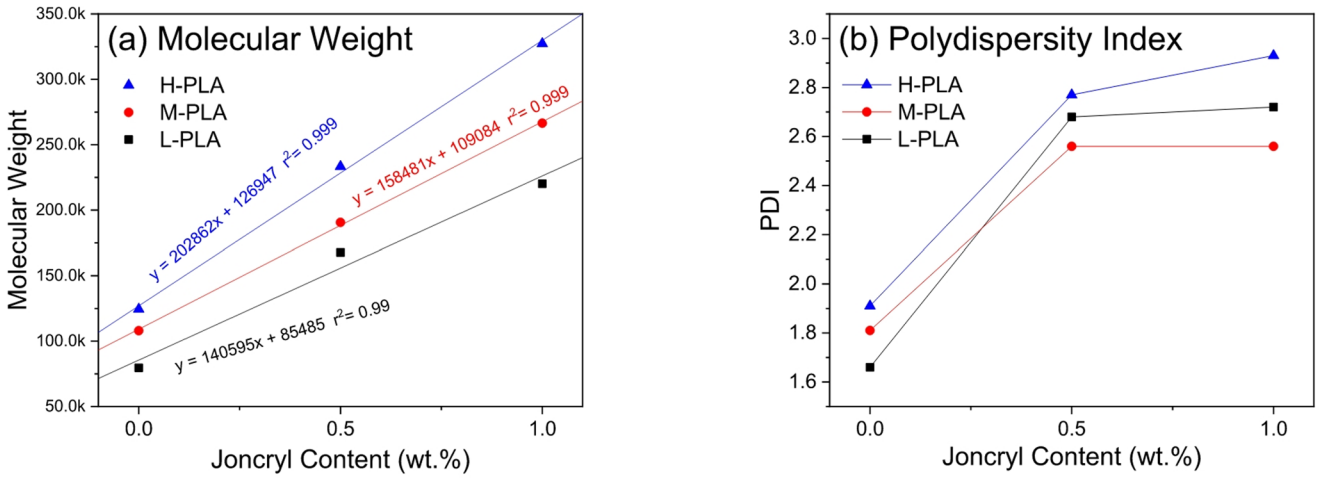

Fig. 7 GPC analysis of all processed samples: (**a**) molecular weight and, (**b**) *PDI*

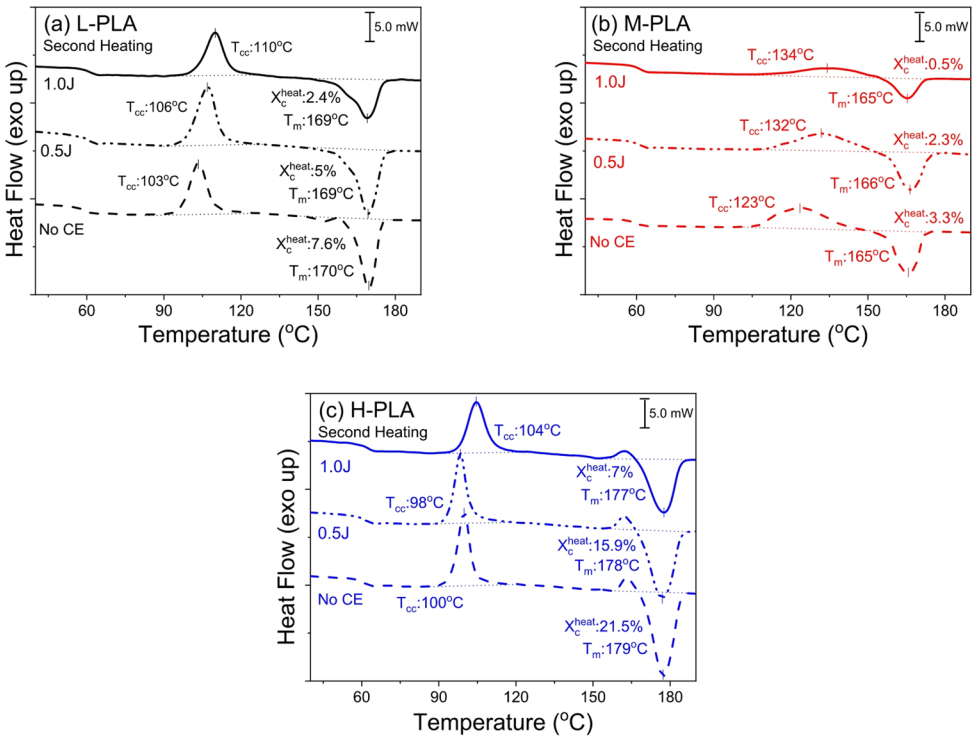

Fig. 8 Second heating thermograms of (**a**) L-PLA, (**b**) M-PLA and (**c**) H-PLA of all processed samples, recorded at a heating rate of 10 °C/min after cooling at 30 °C/min (cooling curves not shown)

exothermic peak prior to melting (α′-to-α phase transition) was also observed, which is typical of PLA homopolymers with incomplete or low-temperature crystallization [58]. In this study, the rapid cooling rate limited chain mobility, preventing the formation of fully order crystal and leading to incomplete crystallization. The addition of Joncryl generally shifted the cold crystallization temperature to higher values due to the restricted molecular mobility caused by branched structures. This effect was more pronounced in L-PLA (103 °C to 110 °C) and M-PLA (123 °C to 134 °C) than in H-PLA (100 °C to 104 °C). An exception was observed for H-PLA with 0.5 wt% Joncryl, where the cold crystallization peak appeared earlier, at 98 °C. This behavior may be attributed to the nucleating effect of the branched structures in highly crystallizable H-PLA, which facilitates the onset of crystallization at low Joncryl content [20, 26]. A similar effect was observed in L-PLA, where the enthalpy of cold crystallization increased from 29.1 to 37.1 J/g which is followed by a reduction after 1.0 wt% Joncryl addition (Table 5), indicating more crystallization occurred with 0.5 wt% Joncryl addition in nucleation-dominated crystallization temperatures. This indicates that a small amount of branching can enhance crystallization in PLAs with lower molecular weight and D-content.

Table 5 Second heating DSC thermograms summary of fast cooled processed samples

Samples	T_{cc} (°C)	ΔH_{cc} (J/g)	T_m (°C)	ΔH_m (J/g)	X_c^{heat} %
L-PLA					
No CE	103	29.1	170	36.3	7.7
0.5 J	106	37.1	169	41.8	5.0
1.0 J	110	30.5	169	32.8	2.4
M-PLA					
No CE	123	29.8	165	32.9	3.3
0.5 J	132	23.2	166	25.4	2.3
1.0 J	234	12	165	12.5	0.5
H-PLA					
No CE	100	33.1	179	53.3	21.6
0.5 J	98	30.2	178	45.1	15.9
1.0 J	104	27.6	177	34.2	7.0

Figure 9 presents the slow-cooling (2 °C/min) and subsequent second heating thermograms of all processed samples, with quantitative results summarized in Table 6. This slow cooling rate was applied to maximize melt crystallization and to investigate the effect of Joncryl-induced branching on non-isothermal melt crystallization behavior. Figure 9a–c shows that crystallization in unmodified H-PLA occurred earlier and exhibited a higher degree of crystallinity than in the other PLAs, due to its lower D-content [54]. While Joncryl modification reduced the overall degree of crystallinity in all samples, the melt crystallization temperature (T_c) of L-PLA and M-PLA remained largely unchanged. On the other hand, melt crystallization temperature of H-PLA decreased from 116 °C to 104 °C after 1.0 wt% Joncryl addition. This behavior can be attributed to the synergistic effect of low D-content and Joncryl-induced branching, where the high crystallizability of low D-content PLA and the nucleating effect of branches promote faster and more extensive crystallization during cooling. While this leads to a lower T_c value where crystallization continues as lower temperatures, the resulting crystals are less perfect which is reflected as lower ΔH_m and T_m values.

Figure 10 illustrates the isothermal crystallization behavior of unmodified (Fig. 10a) and 1.0 wt% Joncryl-modified (Fig. 10b) PLA samples, investigated at temperatures ranging from 90 to 120 °C. The crystallization half-times, defined as the time required to reach 50% of the final crystallinity during isothermal treatment, are presented in Fig. 10a′-b′ for unmodified and Joncryl-modified samples, respectively. Figure 10a″-b″ show the total crystallinity of unmodified and modified samples throughout the isothermal analysis. H-PLA crystallized faster than L-PLA and M-PLA in both unmodified and modified samples, due to its low D-content. Lower molecular weight of L-PLA also enabled faster crystallization than M-PLA where D-content was same. Joncryl modification approximately doubled the crystallization half-times in all samples, as branching hindered the chain mobility required for crystallization. This effect was more pronounced at lower isothermal temperatures, where molecular mobility and crystal growth rates are lower [16, 46], and in higher D-content samples (L-PLA and M-PLA), where crystal formation is inherently slower in linear chains [26, 48], as also observed in Fig. 9. Figure 10a′–b′ show that crystallization was fastest between 100 and 110 °C, whereas it was slowest at 90 °C due to nucleation-dominated crystallization combined with limited molecular mobility [59, 60]. Figure 10a″–b″ indicate that unmodified samples achieved higher overall crystallinity than their modified counterparts, as linear, lower-molecular-weight chains crystallize more easily than branched, bulkier chains.

Table 7 presents the Avrami kinetic parameters calculated from the isothermal crystallization data. Detailed graphs of relative crystallinity curves at all temperatures (Figure S4), relative crystallinity curves at 100 °C and 110 °C (Figure S5), Avrami double-log plots (Figure S6), and isothermal crystallization rates (Figure S7) are provided in the Supplementary Data. As shown in the relative crystallinity curves (Figures S4–S5), all unmodified samples crystallized faster than their Joncryl-modified counterparts. This behavior is attributed to increased molecular weight and long-chain branching in the modified samples, which reduce chain mobility and limit chain foldability. Despite its higher molecular weight, H-PLA crystallized faster than L-PLA and M-PLA due to its lower D-content. Figure S6 indicates that the Avrami exponent (n) values range between 2 and 3 for all samples, suggesting that crystallization predominantly occurs as two-dimensional spherulites. Figure S7 shows distinct differences in the crystallization rate constant (k) values among unmodified samples: H-PLA ($k_{max} \approx 100$), M-PLA ($k_{max} \approx 4$), and L-PLA ($k_{max} \approx 6.5$). Joncryl modification produced a similar trend but with substantially reduced k values. These results highlight the influence of D-content on crystallization rate and explain the absence of cold crystallization in H-PLA observed in Fig. 9c′. For samples with the same D-content, L-PLA exhibited higher k values than M-PLA, demonstrating the effect of molecular

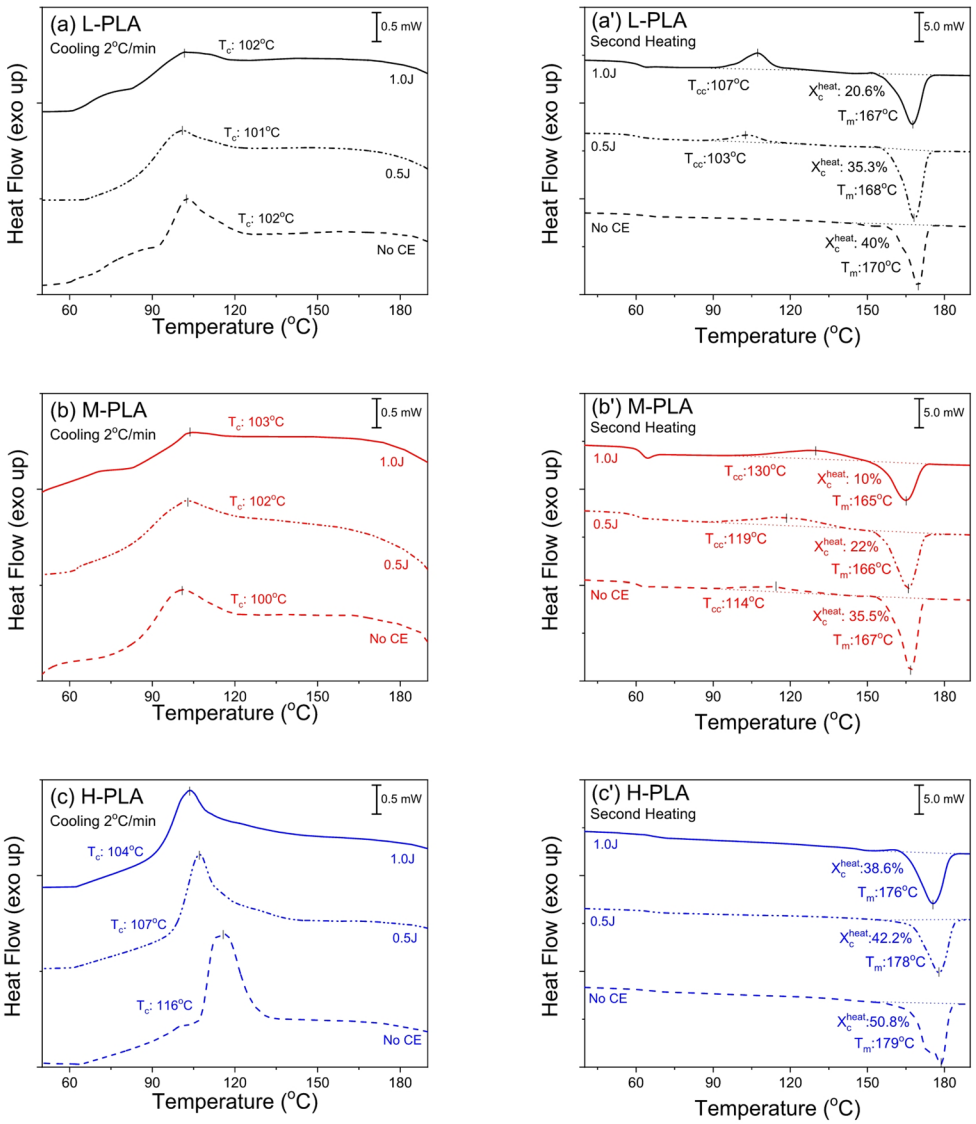

Fig. 9 Thermograms of (**a**, **b**, **c**) cooling and (**a′**, **b′**, **c′**) second heating of all processed samples at cooling rate of 2 °C/min and heating rate of 10 °C/min

Table 6 Slow cooling and second heating DSC thermogram summary of processed samples

Samples	T_c (°C)	T_{cc} (°C)	ΔH_{cc} (J/g)	T_m (°C)	ΔH_m (J/g)	X_c^{heat} (%)
L-PLA						
No CE	102	-	-	170	37.5	40.1
0.5 J	101	103	5.13	168	38.2	35.3
1.0 J	102	107	10.7	167	30.0	20.6
M-PLA						
No CE	100	114	3.6	167	36.9	35.6
0.5 J	102	119	11.8	166	32.4	22.0
1.0 J	103	130	13.9	165	23.3	10.0
H-PLA						
No CE	116	-	-	179	47.6	50.8
0.5 J	107	-	-	178	39.5	42.2
1.0 J	104	-	-	176	36.2	38.7

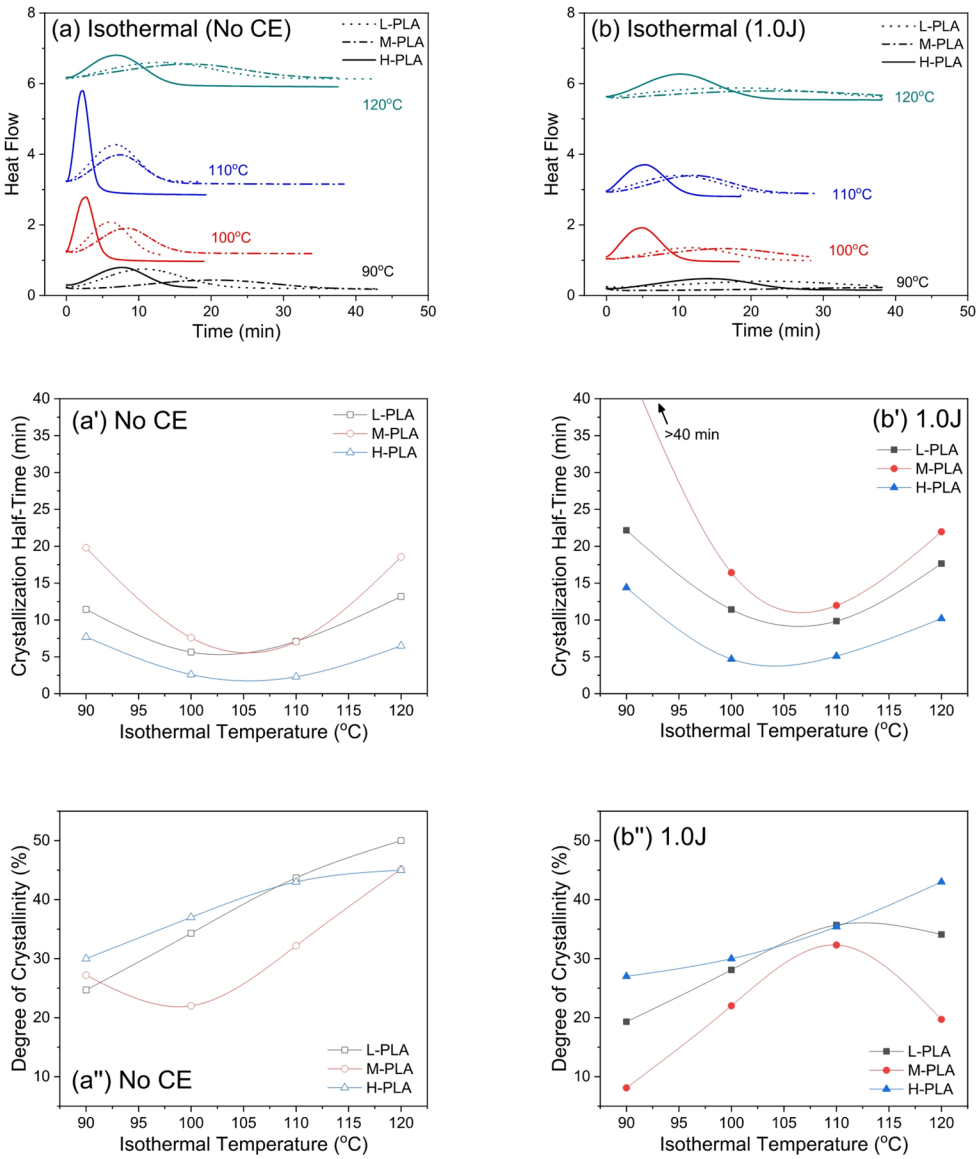

Fig. 10 Isothermal melt crystallization, crystallization half-times, and total crystallinity of (**a**, **a′**, **a″**) unmodified and (**b**, **b′**, **b″**) Joncryl modified processed samples

weight and explaining the lack of cold crystallization of L-PLA in unmodified sample shown in Fig. 9a′–b′. Overall, the Avrami analysis aligns well with previous studies on the isothermal crystallization kinetics of different PLAs and PLA-based systems [13, 46, 61–64].

Conclusion

This study demonstrated that the effectiveness of Joncryl modification is strongly influenced by the molecular weight of PLA. Higher-molecular-weight PLA (H-PLA) exhibited a more pronounced increase in complex viscosity compared to lower-molecular-weight PLA (L-PLA). Time-weighted relaxation spectra, Cole–Cole and, Van-Gurp Palmen analyses further confirmed that reductions in the storage modulus (G′) slope were associated with the extent of chain branching, with H-PLA being affected the most. These results indicate that higher initial molecular weights lead to stronger branch interactions after Joncryl modification. GPC analysis corroborated that the increase in molecular weight upon Joncryl modification correlated linearly with the amount of Joncryl added, demonstrating that chain branching is more effective in enhancing the rheological and thermal properties of higher-molecular-weight PLAs.

The crystallization kinetics of all PLA samples were also influenced by Joncryl. Both crystallization times and total crystallinity decreased relative to the unmodified samples. Non-isothermal and isothermal analyses showed that Joncryl modification significantly reduced crystallinity, particularly at 1.0 wt% Joncryl. Non-isothermal analysis revealed that cold crystallization temperatures increased with Joncryl

Table 7 Avrami kinetic parameters of all processed samples

Samples		T (°C)	k ($x10^{-3}$ min^{-n})	*n*	$1/t_{0.5}$ (min^{-1})	$\tau_{1/2}$ (min^{-1})	R^2
L-PLA	No CE	90	1.93	2.48	0.093	0.093	>0.990
		100	5.87	2.74	0.172	0.175	
		110	5.91	2.50	0.147	0.149	
		120	1.71	2.32	0.074	0.075	
	1.0 J	90	0.27	2.61	0.049	0.050	
		100	1.43	2.57	0.088	0.090	
		110	2.81	2.39	0.098	0.100	
		120	1.34	2.20	0.056	0.058	
M-PLA	No CE	90	0.24	2.72	0.053	0.054	
		100	3.95	2.59	0.134	0.136	
		110	3.37	2.68	0.136	0.137	
		120	1.00	2.35	0.061	0.062	
	1.0 J	90	-	-	-	-	
		100	0.77	2.52	0.067	0.067	
		110	1.32	2.56	0.085	0.087	
		120	0.89	2.27	0.052	0.053	
H-PLA	No CE	90	2.25	2.81	0.130	0.130	
		100	47.1	2.53	0.344	0.346	
		110	100.8	2.49	0.435	0.461	
		120	5.08	2.57	0.143	0.148	
	1.0 J	90*	0.75	2.57	0.068	0.070	
		100*	13.0	2.63	0.215	0.220	
		110*	18.7	2.66	0.254	0.257	
		120*	6.05	2.65	0.168	0.167	

content in all samples, except for H-PLA with 0.5 wt% Joncryl, indicating that low D-content PLAs can benefit from small amounts of branching. Similarly, L-PLA with 0.5 wt% Joncryl also exhibited higher crystallization. Isothermal analysis demonstrated that the addition of Joncryl nearly doubled the crystallization half-times and reduced the overall crystallinity of all samples, regardless of molecular weight. Avrami analysis of the isothermal data showed that the crystallization rate constant of H-PLA was much higher than that of L-PLA and M-PLA, owing to its lower D-content. L-PLA exhibited a higher rate constant than M-PLA, reflecting the influence of molecular weight. Joncryl modification significantly reduced the crystallization rate constants in all samples, further confirming the impact of chain branching on PLA crystallization behavior.

Supplementary Information The online version contains supplementary material available at https://doi.org/10.1007/s10924-025-03753-8.

Acknowledgements Authors would also like to acknowledge Istanbul Technical University Scientific Research Project (ITU-BAP) for the financial support with the project number 43944. Authors also thank the financial support of University of Bonab (project number 140402). We would like to thank Burcu Özdemir, Andreas Himmelsbach, and Selen Kader to help running part of the experiments.

Author Contributions Y.A: Writing – original draft, Methodology, Investigation, Formal analysis, Data curation. M.B.A.: Methodology, Investigation, Formal analysis, Data curation. J.R.: Formal analysis, Data curation. M.G.: Formal analysis, Data curation. A.D.: Visualization, Validation, Resources, Methodology. D. J.: Visualization, Validation, Resources, Methodology, Funding acquisition. M. N.: Writing – review & editing, Visualization, Validation, Supervision, Project administration, Methodology, Investigation, Funding acquisition, Formal analysis, Conceptualization.

Funding Open access funding provided by the Scientific and Technological Research Council of Türkiye (TÜBİTAK).

Data Availability No datasets were generated or analysed during the current study.

Declarations

Competing Interests The authors declare no competing interests.

Open Access This article is licensed under a Creative Commons Attribution 4.0 International License, which permits use, sharing, adaptation, distribution and reproduction in any medium or format, as long as you give appropriate credit to the original author(s) and the source, provide a link to the Creative Commons licence, and indicate if changes were made. The images or other third party material in this article are included in the article's Creative Commons licence, unless indicated otherwise in a credit line to the material. If material is not included in the article's Creative Commons licence and your intended use is not permitted by statutory regulation or exceeds the permitted use, you will need to obtain permission directly from the copyright holder. To view a copy of this licence, visit http://creativecommons.org/licenses/by/4.0/.

References

1. Gironi F, Piemonte V (2011) Bioplastics and petroleum-based plastics: strengths and weaknesses. Energy Sour Part A Recover Util Environ Eff 33(21):1949–1959. https://doi.org/10.1080/15567030903436830
2. Tokiwa Y, Calabia BP (2007) Biodegradability and biodegradation of polyesters. J Polym Environ 15(4):259–267. https://doi.org/10.1007/s10924-007-0066-3
3. Dorgan JR, Lehermeier HJ, Palade L-I, Cicero J (2001) Polylactides: properties and prospects of an environmentally benign plastic from renewable resources. Macromol Symp 175(1):55–66
4. Garlotta D (2001) A literature review of poly (lactic acid). J Polym Environ 9(2):63–84. https://doi.org/10.1023/A:1020200822435
5. Palade L-I, Lehermeier HJ, Dorgan JR (2001) Melt rheology of high L-content poly(lactic acid). Macromolecules 34(5):1384–1390. https://doi.org/10.1021/ma001173b
6. Auras R, Harte B, Selke S (2004) An overview of polylactides as packaging materials. Macromol Biosci 4(9):835–864. https://doi.org/10.1002/mabi.200400043
7. Gupta B, Revagade N, Hilborn J (2007) Poly(lactic acid) fiber: an overview. Prog Polym Sci 32(4):455–482. https://doi.org/10.1016/j.progpolymsci.2007.01.005
8. Lim L-T, Auras R, Rubino M (2008) Processing technologies for poly(lactic acid). Prog Polym Sci 33(8):820–852. https://doi.org/10.1016/j.progpolymsci.2008.05.004
9. Auras R (2010) Poly(lactic acid). Encycl Polym Sci Technol. https://doi.org/10.1002/0471440264.pst275
10. Saeidlou S, Huneault MA, Li H, Park CB (2012) Poly(lactic acid) crystallization. Prog Polym Sci 37(12):1657–1677. https://doi.org/10.1016/j.progpolymsci.2012.07.005
11. Ajioka M, Enomoto K, Suzuki K, Yamaguchi A (1995) Basic properties of polylactic acid produced by the direct condensation polymerization of lactic acid. Bull Chem Soc Jpn 68(8):2125–2131. https://doi.org/10.1246/bcsj.68.2125
12. Nofar M, Salehiyan R, Sinha Ray S (2019) Rheology of poly (lactic acid)-based systems. Polym Rev 59(3):465–509. https://doi.org/10.1080/15583724.2019.1572185
13. Pantani R, De Santis F, Sorrentino A, De Maio F, Titomanlio G (2010) Crystallization kinetics of virgin and processed poly(lactic acid). Polym Degrad Stab 95(7):1148–1159. https://doi.org/10.1016/j.polymdegradstab.2010.04.018
14. McKee MG, Unal S, Wilkes GL, Long TE (2005) Branched polyesters: recent advances in synthesis and performance. Prog Polym Sci 30(5):507–539. https://doi.org/10.1016/j.progpolymsci.2005.01.009
15. Michalski A, Brzezinski M, Lapienis G, Biela T (2019) Star-shaped and branched polylactides: synthesis, characterization, and properties. Prog Polym Sci 89:159–212. https://doi.org/10.1016/j.progpolymsci.2018.10.004
16. Göttermann S, Standau T, Weinmann S, Altstädt V, Bonten C (2017) Effect of chemical modification on the thermal and rheological properties of polylactide. Polym Eng Sci. https://doi.org/10.1002/pen.24505
17. Li H, Huneault MA (2011) Effect of chain extension on the properties of PLA/TPS blends. J Appl Polym Sci 122(1):134–141. https://doi.org/10.1002/app.33981
18. Standau T, Zhao C, Murillo Castellón S, Bonten C, Altstädt V (2019a) Chemical modification and foam processing of polylactide (PLA). Polymers 11(2):306. https://doi.org/10.3390/polym11020306
19. Standau T, Castellón SM, Delavoie A, Bonten C, Altstädt V (2019b) Effects of chemical modifications on the rheological and the expansion behavior of polylactide (PLA) in foam extrusion. E-Polymers 19(1):297–304. https://doi.org/10.1515/epoly-2019-0030
20. Nofar M, Zhu W, Park CB, Randall J (2011) Crystallization kinetics of linear and long-chain-branched polylactide. Ind Eng Chem Res 50(24):13789–13798. https://doi.org/10.1021/ie2011966
21. Corre Y-M, Maazouz A, Reignier J, Duchet J (2013) Influence of the chain extension on the crystallization behavior of polylactide. Polym Eng Sci 54(3):616–625. https://doi.org/10.1002/pen.23595
22. Najafi N, Heuzey MC, Carreau PJ, Wood-Adams PM (2012a) Control of thermal degradation of polylactide (PLA)-clay nanocomposites using chain extenders. Polym Degrad Stab 97(4):554–565. https://doi.org/10.1016/j.polymdegradstab.2012.01.016
23. Najafi N, Heuzey MC, Carreau PJ (2012b) Crystallization behavior and morphology of polylactide and PLA/clay nanocomposites in the presence of chain extenders. Polym Eng Sci 53(5):1053–1064. https://doi.org/10.1002/pen.23355
24. Gu SY, Yang M, Yu T, Ren TB, Ren J (2008) Synthesis and characterization of biodegradable lactic acid-based polymers by chain extension. Polym Int 57(8):982–986. https://doi.org/10.1002/pi.2435
25. Mihai M, Huneault MA, Favis BD (2009) Rheology and extrusion foaming of chain-branched poly(lactic acid). Polym Eng Sci 50(3):629–642. https://doi.org/10.1002/pen.21561
26. Akdevelioğlu Y, Begum Alanalp M, Siyahcan F, Randall J, Gehrung M, Durmus A, Nofar M (2024) Joncryl chain extender reactivity with polylactide: effect of d-lactide content, Joncryl type, and processing temperature. J Rheol 68(2):247–262. https://doi.org/10.1122/8.0000718
27. Dorgan JR, Williams JS, Lewis DN (1999) Melt rheology of poly(lactic acid): entanglement and chain architecture effects. J Rheol 43(5):1141–1155. https://doi.org/10.1122/1.551041
28. Meng Q, Heuzey M-C, Carreau PJ (2012) Control of thermal degradation of polylactide/clay nanocomposites during melt processing by chain extension reaction. Polym Degrad Stab 97(10):2010–2020. https://doi.org/10.1016/j.polymdegradstab.2012.01.030
29. Perego G, Cella GD, Bastioli C (1996) Effect of molecular weight and crystallinity on poly(lactic acid) mechanical properties. J Appl Polym Sci 59(1):37–43. https://doi.org/10.1002/(sici)1097-4628(19960103)59:1<37::aidapp6>3.3.co;2-7
30. Najafi N, Heuzey M-C, Carreau PJ, Therriault D, Park CB (2014) Rheological and foaming behavior of linear and branched polylactides. Rheol Acta 53(10–11):779–790. https://doi.org/10.1007/s00397-014-0801-3
31. Tuna B, Ozkoc G (2016) Effects of diisocyanate and polymeric epoxidized chain extenders on the properties of recycled poly(lactic acid). J Polym Environ 25(4):983–993. https://doi.org/10.1007/s10924-016-0856-6
32. Barletta M, Aversa C, Puopolo M (2020) Recycling of PLA-based bioplastics: the role of chain-extenders in twin-screw extrusion compounding and cast extrusion of sheets. J Appl Polym Sci. https://doi.org/10.1002/app.49292
33. Li M, Li S, Liu B, Jiang T, Zhang D, Cao L, He L, Gong W (2021) Rheological behavior, crystallization properties, and foaming performance of chain-extended Poly (lactic acid) by functionalized epoxy. RSC Adv 11(52):32799–32809. https://doi.org/10.1039/d1ra06382k
34. Zhao X, Pelfrey A, Pellicciotti A, Koelling K, Vodovotz Y (2023) Synergistic effects of chain extenders and natural rubber on PLA thermal, rheological, mechanical and barrier properties. Polymer 269:125712. https://doi.org/10.1016/j.polymer.2023.125712
35. Li L, Wang H, Jiang T, Hu C, Zhang J, Zheng H, Zeng G (2023) Effect of epoxy chain extenders on molecular structure and properties of polylactic acid. J Appl Polym Sci. https://doi.org/10.1002/app.54379

36. Sun H, Luo W, Weng Y, Zhang C (2025) Advances in poly(lactic acid) chain extenders: mechanisms, performance, and sustainability. J Vinyl Addit Technol. https://doi.org/10.1002/vnl.70032
37. Nouri S, Dubois C, Lafleur PG (2015) Effect of chemical and physical branching on rheological behavior of polylactide. J Rheol 59(4):1045–1063. https://doi.org/10.1122/1.4922486
38. Gu L, Xu Y, Fahnhorst GW, Macosko CW (2017) Star vs long chain branching of poly(lactic acid) with multifunctional Aziridine. J Rheol 61(4):785–796. https://doi.org/10.1122/1.4985344
39. Villalobos M, Awojulu A, Greeley T, Turco G, Deeter G (2006) Oligomeric chain extenders for economic reprocessing and recycling of Condensation Plastics. Energy 31(15):3227–3234. https://doi.org/10.1016/j.energy.2006.03.026
40. Cailloux J, Santana OO, Maspoch M. Ll., Bou JJ, Carrasco F (2015) Using viscoelastic properties to quantitatively estimate the amount of modified poly(lactic acid) chains through reactive extrusion. J Rheol 59(5):1191–1227. https://doi.org/10.1122/1.4928071
41. Standau T, Nofar M, Dörr D, Ruckdäschel H, Altstädt V (2021) A review on multifunctional epoxy-based Joncryl® ADR chain extended thermoplastics. Polym Rev 62(2):296–350. https://doi.org/10.1080/15583724.2021.1918710
42. Nofar M, Oğuz H (2019) Development of PBT/recycled-pet blends and the influence of using chain extender. J Polym Environ 27(7):1404–1417. https://doi.org/10.1007/s10924-019-01435-w
43. Akdevelioğlu Y, Himmelsbach A, Ruckdäschel H, Nofar M (2024) Melt rheological and bead foaming behavior of recycled polyethylene terephthalate/polybutylene terephthalate blends modified with a Joncryl chain extender. Ind Eng Chem Res 63(14):6222–6234. https://doi.org/10.1021/acs.iecr.3c03371
44. Härth M, Dörnhöfer A, Kaschta J, Münstedt H, Schubert DW (2020) Molecular structure and rheological properties of a poly(ethylene terephthalate) modified by two different chain extenders. J Appl Polym Sci 138(13). https://doi.org/10.1002/app.50110
45. Guclu M, Göksu YA, Özdemir B, Ghanbari A, Nofar MR (2021) Thermal stabilization of recycled pet through chain extension and blending with PBT. https://doi.org/10.21203/rs.3.rs-505084/v1
46. Bai J, Fang H, Zhang Y, Wang Z (2014) Studies on crystallization kinetics of bimodal long chain branched polylactides. CrystEngComm 16(12):2452. https://doi.org/10.1039/c3ce42319k
47. Bigg DM (2005) Polylactide copolymers: effect of copolymer ratio and end capping on their properties. Adv Polym Technol 24(2):69–82. https://doi.org/10.1002/adv.20032
48. Kolstad JJ (1996) Crystallization kinetics of poly(L-Lactide-co-meso-lactide). J Appl Polym Sci 62(7):1079–1091. https://doi.org/10.1002/(sici)1097-4628(19961114)62:7<1079::aid-app14>3.0.co;2-1
49. Zirak N, Shirinbayan M, Farzaneh S, Tcharkhtchi A (2022) Effect of molecular weight on crystallization behavior of poly (lactic acid) under isotherm and non-isotherm conditions. Polym Adv Technol 33(4):1307–1316. https://doi.org/10.1002/pat.5603
50. Yang H, Du J (2023) Crystallinity, rheology, and mechanical properties of low-/high-molecular-weight PLA blended systems. Molecules 29(1):169. https://doi.org/10.3390/molecules290101691
51. Migliaresi C, Cohn D, De Lollis A, Fambri L (1991) Dynamic mechanical and calorimetric analysis of compression-molded plla of different molecular weights: effect of thermal treatments. J Appl Polym Sci 43(1):83–95. https://doi.org/10.1002/app.1991.070430109
52. Atalay SE, Bezci B, Özdemir B, Göksu YA, Ghanbari A, Jalali A, Nofar M (2021) Thermal and environmentally induced degradation behaviors of amorphous and semicrystalline Plas through rheological analysis. J Polym Environ 29(10):3412–3426. https://doi.org/10.1007/s10924-021-02128-z
53. Fischer EW, Sterzel HJ, Wegner G (1973) Investigation of the structure of solution grown crystals of lactide copolymers by means of chemical reactions. Kolloid-Zeitschrift Und Zeitschrift Für Polymere 251(11):980–990. https://doi.org/10.1007/bf01498927
54. Nofar M (2021) Multiphase polylactide blends towards a sustainable and green environment. Elsevier
55. Avrami M (1939) Kinetics of phase change. I general theory. J Chem Phys 7(12):1103–1112. https://doi.org/10.1063/1.1750380
56. Corre Y-M, Duchet J, Reignier J, Maazouz A (2011) Melt strengthening of poly (lactic acid) through reactive extrusion with epoxy-functionalized chains. Rheol Acta 50(7–8):613–629. https://doi.org/10.1007/s00397-011-0538-1
57. Dorgan JR, Janzen J, Clayton MP, Hait SB, Knauss DM (2005) Melt rheology of variable l-content poly(lactic acid). J Rheol 49(3):607–619. https://doi.org/10.1122/1.1896957
58. Pan P, Zhu B, Kai W, Dong T, Inoue Y (2008) Polymorphic transition in disordered poly(l-lactide) crystals induced by annealing at elevated temperatures. Macromolecules 41(12):4296–4304. https://doi.org/10.1021/ma800343g
59. Foglia F, De Meo A, Iozzino V, Volpe V, Pantani R (2020) Isothermal crystallization of PLA: nucleation density and growth rates of α and α' phases. Can J Chem Eng 98(9):1998–2007. https://doi.org/10.1002/cjce.23818
60. Ma B, Wang X, He Y, Dong Z, Zhang X, Chen X, Liu T (2021) Effect of poly(lactic acid) crystallization on its mechanical and heat resistance performances. Polymer 212:123280. https://doi.org/10.1016/j.polymer.2020.123280
61. Peng Q, Li S, Liu F, Li G, Liao X (2024) Effect of the interchain interaction on the crystallization kinetics and crystal structure of polylactic acid under nitrogen. CrystEngComm 26(42):6082–6090. https://doi.org/10.1039/d4ce00767k
62. Mat Taib R, Tham CY (2017) Isothermal crystallization kinetics and spherulite morphologies of poly(lactic acid)/ethylene acrylate copolymer blends. J Appl Polym Sci. https://doi.org/10.1002/app.45487
63. Refaa Z, Boutaous M, Siginer DA (2018) PLA crystallization kinetics and morphology development. Int Polym Proc 33(3):336–344. https://doi.org/10.3139/217.3525
64. Zhu Y, Zhang X, Jia S, Yan Z, Liang W, Zhang Y, Coates P, Liu W (2024) Recent reviews for isothermal crystallization kinetics and its regulation strategies of PLA. J Polym Res. https://doi.org/10.1007/s10965-024-04096-z

Publisher's Note Springer Nature remains neutral with regard to jurisdictional claims in published maps and institutional affiliations.